JOURNAL OF MATERIALS SCIENCE 22 (1987) 4002–4010

The longitudinal electrical conductivity of metal matrix composites at cryogenic temperature in the presence of a longitudinal magnetic field

PART 2 *Application of the solution to metal matrix composites*

FRANCESC S. ROIG
College of Creative Studies, University of California, Santa Barbara, California 93106, USA
JACQUES E. SCHOUTENS*
MMCIAC, Kaman Tempo, 816 State Street, Santa Barbara, California 93102, USA

In this paper we use the results of Part I to derive two integral expressions for the electrical conductivity of metal matrix composite materials when a magnetic field, B, is added to a small electric field also parallel to fibres. One expression applies to strong magnetic fields meaning $R_0/a < 1$, where $R_0 = m^*v_F/eB$ when the Fermi velocity is perpendicular to the magnetic field. When $B \rightarrow \infty$, the integral expression reduces to the well known conductivity value $\sigma = \sigma_0(1 - V_f)$, where σ_0 is the bulk matrix conductivity and V_f is the fibre volume fraction. For weak magnetic fields, $R_0/a > 1$, then the electrical conductivity is expressed by the sum of two integrals. When $B \rightarrow 0$, the electrical conductivity reduces to the integral expression obtained in our earlier results when there is only a longitudinal electric field. In this paper we correct an incorrect derivation of the composite conductivity in the absence of a magnetic field published earlier [J. Mater. Sci. **21** (1986) 2409].

1. Introduction

This is the second part of two papers on the effects of magnetic fields on the electrical conductivity of metal matrix composite (MMC) materials. The electric and magnetic fields are assumed to be parallel to the fibres. In the first paper [1], we found the solution of the Boltzmann equation for the case of cylindrical fibres. It was assumed that the scattering regions for adjacent fibres do not overlap.

In the present paper we construct an integral expression for the electrical conductivity of MMC materials. This expression is based on the solution of the Boltzmann equation discussed before [1], and is shown to have the appropriate behaviour in the limit, that is, for very large magnetic fields the conductivity goes to the bulk value. This follows from the fact that at extremely high magnetic fields the radius of curvature of the electron trajectories is extremely small so that the scattering effect of the fibres is negligible. For very small magnetic fields, the expression for the electrical conductivity in the presence of an electric field only is recovered. This follows from the fact that the very small magnetic fields have a negligible effect upon the electron trajectories.

To find the electrical conductivity we need to integrate at each point in the metal matrix over all possible directions of the velocity. The possible trajectories are those for which the electron paths emerge from the fibre surfaces. In essence, this will determine the limits of the integrations to be performed, which is the main task described in this paper. The integration over all possible velocity directions is done first by integrating over the azimuthal angle ϕ and then over the polar angle θ, that the velocity makes with the fibre axis (z-axis). For a given magnetic field the radius of curvature of the electron trajectories in the plane transverse to the fibres depends on the angle θ. Then for a given radius the possible value of ϕ are determined by tangency conditions of the circular trajectory and the fibre. In the next section we study these tangency conditions. In this paper, we use the same notation as we used in Part I [1].

2. The solution of the Boltzmann equation and the tangency conditions

In Part I we showed that the solution of the Boltzmann equation, when a longitudinal magnetic field is present, is

$$F^1 = A\{1 - e^{-\psi/\omega_0\tau}\} \quad (1)$$

where A is constant, ω_0 is the angular frequency of the electrons when the magnetic field is present and τ is the relaxation time, and F^1 is the change in the equilibrium distribution function. The expression for ψ was

*To whom correspondence should be addressed.

0022–2461/87 $03.00 + .12

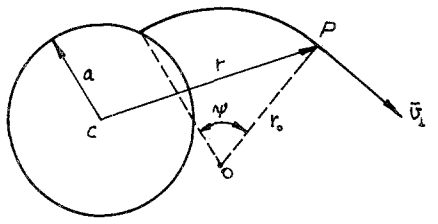

Figure 1 Trajectory of electrons scattered from fibre surface when $r_0 > a$. (In this, and all subsequent figures unless otherwise stated, the magnetic field is directed into the paper.)

found to be $\psi = \alpha - \delta$, where

$$\alpha = \sin^{-1}\left\{\frac{\omega_0 r v_r}{[(v_r^2 + v_\varphi^2)(v_r^2 + v_\varphi^2 + 2\omega_0 r v_\varphi + \omega_0^2 r^2)]^{1/2}}\right\} \tag{2a}$$

$$\delta = \sin^{-1}\left\{\frac{\omega_0[a^2(v_r^2 + v_\varphi^2) - (rv_\varphi + \frac{1}{2}\omega_0(r^2 - a^2))^2]^{1/2}}{[(v_r^2 + v_\varphi^2)(v_r^2 + v_\varphi^2 + 2\omega_0 r v_\varphi + \omega_0^2 r^2)]^{1/2}}\right\} \tag{2b}$$

where a is the fibre radius. The angle ψ is shown in Fig. 1. The radius of the electron trajectory is r_0 with

$$r_0 = \frac{v}{\omega_0}\sin\theta \tag{3}$$

where θ is the angle between $\bar{v}$ and the z-axis [1].

Two cases must be distinguished: $r_0 < a$ and $r_0 > a$.

2.1. Case $r_0 < a$

From Fig. 2 the tangency condition follows at once, namely $r_c^2 = (r_0 + a)^2 = r^2 + r_0^2 + 2rr_0 \sin\phi_T$

$$\sin\phi_T = -\frac{1}{2}\left(\frac{r^2 - a^2}{rr_0}\right) + \frac{a}{r}. \tag{4}$$

Writing $r_0 = (v_r^2 + v_\varphi^2)^{1/2}/\omega_0$ and $\sin\phi_T = v_\varphi/(v_r^2 + v_\varphi^2)^{1/2}$ it can be checked easily that Equation 4 is equivalent to the vanishing of the numerator in the second term of the second Equation 2 (the angle $\delta = 0$).

Now as Fig. 3 shows we can also have another tangency angle ϕ_T' for a given point P in the metal such that $\sin\phi_T' = \sin\phi_T$ and $\cos\phi_T' = -\cos\phi_T$, that is, ϕ_T corresponds to $v_r > 0$ and ϕ_T' to $v_r < 0$. The two velocities corresponding to ϕ_T and ϕ_T' are symmetrical with respect to the vertical line passing through P. The shaded area, shown in Fig. 3, is the region of integration for ϕ. For any angle ϕ within the shaded region we obtain trajectories that originate at the fibre.

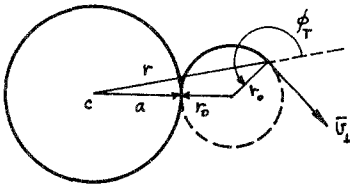

Figure 2 Trajectory of electrons scattered from fibre surface when $r_0 < a$.

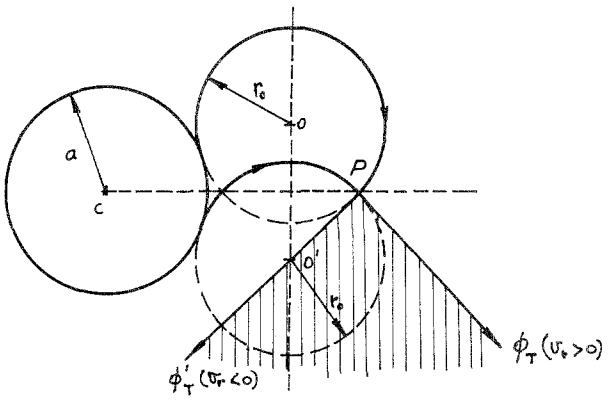

Figure 3 Symmetry conditions for scattering events tangent to fibre surface.

Equation 4 for ϕ_T gives $\phi_T = 0$ at $r = \sqrt{a(2r_0 + a)}$, $\sin\phi_T > 0$ for $a < r < [a(2r_0 + a)]^{1/2}$ and $\sin\phi_T < 0$ for $[a(2r_0 + a)]^{1/2} < r < 2r_0 + a$. At $r = 2r_0 + a$ we obtain $\phi_T = \phi_T' = 3\pi/2$. These results are shown in Fig. 4. For $r > 2r_0 + a$, the trajectory does not intersect the fibre and $\psi = \infty$, and thus produces no change in the bulk distribution function (Equation 1).

For a given radial distance r, there is a relation between ψ corresponding to $\bar{v} = \bar{v}(v_r, v_\varphi)$ and ψ' corresponding to $\bar{v}_T' = \bar{v}(-v_r, v_\varphi)$.

This is shown in Fig. 5. We have that $\psi' = 2(\pi - \delta) - \psi$, and $\psi = \alpha - \delta$, then,

$$\psi' = 2\pi - (\alpha + \delta) \tag{5}$$

This is a useful relation allowing us to integrate ϕ from $\phi = -\pi/2$ to $\phi = \phi_T$ only.

2.2. Case $r_0 > a$

From Fig. 6, we see that we have two possibilities for the tangency condition: $r_c = r_0 \pm a$ or $(r_0 \pm a)^2 = r^2 + r_0^2 + 2rr_0 \sin\phi_T$,

$$\sin\phi_{T\pm} = -\frac{1}{2}\left(\frac{r^2 - a^2}{rr_0}\right) \pm \frac{a}{r} \tag{6}$$

This occurs when $a < r < 2r_0 - a$, because then $\sin\phi_{T\pm} < 1$ as can be readily verified from Equation 6. When $2r_0 - a < r < 2r_0 + a$, then only ϕ_{T+} is allowed. As in the case of $r_0 < a$, we can also have another tangency angle $\phi_{T\pm}'$ such that $\sin\phi_{T\pm}' = \sin\phi_{T\pm}$ and $\cos\phi_{T\pm}' = -\cos\phi_{T\pm}$. Equation 6 for ϕ_{T+} gives $\phi_{T+} = 0$ at $r = [a(2r_0 + a)]^{1/2}$, $\sin\phi_{T+} > 0$ for $a < r < [a(2r_0 + a)]^{1/2}$, $\sin\phi_{T+} < 0$ for $[a(2r_0 + a)]^{1/2} < 2r_0 + a$. At $r = 2r_0 + a$ we have $\phi_{T+}' = \phi_{T+} = 3\pi/2$. At $r = 2r_0 - a$ we have $\sin\phi_T = -1$. Consequently, for the range $a < r < 2r_0 - a$ we obtain two disconnected regions of integration for ϕ as shown in Fig. 7, and for the range $2r_0 - a < r < 2r_0 + a$ there is only one region. Moreover, for $a < r_0 < 3a/2$, we have that $2r_0 - a < [a(2r_0 + a)]^{1/2}$, and for $3a/2 < r_0$ we have that $[a(2r_0 + a)]^{1/2} < 2r_0 - a$. All these results are shown in Fig. 7.

Fig. 8 shows the disconnected regions of trajectories that originate at the fibre. The situation depicted corresponds to $r < 2r_0 - a$. Figs 9a and b show what happens when $r = 2r_0 - a$ and the cases $a < r_0 < 3a/2$ and $3a/2 < r_0$, respectively. At this value of r the

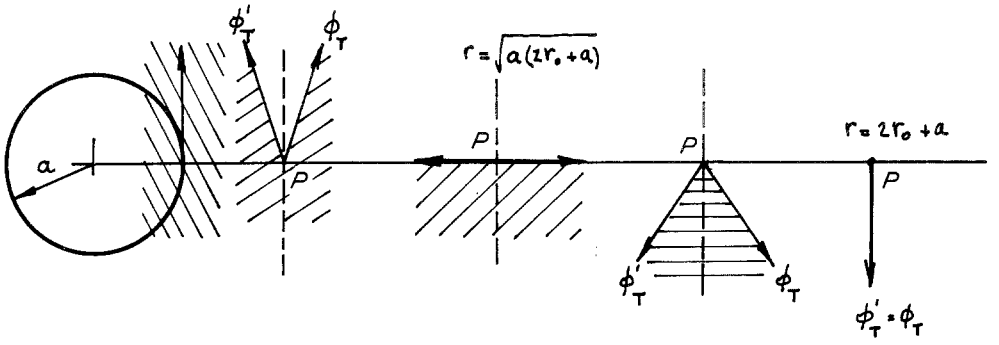

Figure 4 Regions of integration for ϕ as the point P moves away from the fibre surface and $r_0 < a$.

two disconnected integration regions become one. Finally, Fig. 10 shows the general situation when $r > 2r_0 - a$.

The symmetry found for the case $r_0 < a$ also applies to the case when $r_0 > a$. Therefore, we need only integrate ϕ from $-\pi/2$ to ϕ_T.

3. Composite conductivity

Fig. 11 shows a cell in which fibres at four corners represent a well ordered array. This applies to metal matrix composite materials in which the fibres have a relatively large diameter (approximately 0.013 to 0.038 cm), whereas small diameter fibres (approximately 10 μm) are randomly distributed in a plane normal to their longitudinal axis. These array variations are a consequence of material processing which is different for large than for small fibres. In the following analysis we consider only well ordered fibre arrays as shown in Fig. 11, and an extension to other types of arrays has not been made. From Fig. 11, we note that the distance between two nearest fibres is D. We assume that the mean free path Λ for scattering in the bulk metal is such that $\Lambda \leqslant D/2$. In this way there is no overlap between adjacent scattering regions and we can invoke cylindrical symmetry around each fibre.

We denote by A_b the area of the bulk metal not affected by the scattering from nearby fibre surfaces. We denote by A_{sc} area of the scattering region centred on fibres and within a cell. Then we have

$$A_{cell} = A_b + A_{sc} + \pi a^2 \tag{7}$$

which assumes that $A_{sc} = \pi(r_{sc}^2 - a^2)$ and $A_{cell} = (D + 2a)^2$, where r_{sc} is the radius of the scattering region shown in Fig. 11. Now if j_0 denotes the current density in the bulk within a scattering region then the total current within a cell is

$$I = \int_a^{r_{sc}} [j_0 - \Delta j(r)] 2\pi r \, dr + j_0 A_b \tag{8}$$

and the conductivity of the cell is then

$$\sigma = I/EA_{cell} \tag{9}$$

where E is the applied longitudinal electric field. If σ_0 is the conductivity in the bulk area then $j_0 = \sigma_0 E$. It then follows that

$$\frac{\sigma}{\sigma_0} = \left\{\frac{A_{sc} + A_b}{A_{cell}}\right\}\left\{1 - \frac{1}{A_{sc} + A_b}\int_a^{r_{sc}} \frac{\Delta j(r)}{j_0} 2\pi r \, dr\right\} \tag{10a}$$

Using the values for A_{sc}, A_b and A_{cell} we obtain

$$\frac{\sigma}{\sigma_0} = (1 - V_f)\left\{1 - \frac{1}{(1 - V_f)A_{cell}}\int_a^{r_{sc}} \frac{\Delta j(r)}{j_0} 2\pi r \, dr\right\} \tag{10b}$$

Next, we introduce spherical polar coordinates in velocity space

$$v_r = v \sin\theta \cos\phi \tag{11a}$$

$$v_\varphi = v \sin\theta \sin\phi \tag{11b}$$

$$v_z = v \cos\theta. \tag{11c}$$

Then, the Equations 2 for the angles α and δ that define ψ via $\psi = \alpha - \delta$, become

$$\alpha = \sin^{-1}\left\{\frac{\omega_0 r \cos\phi}{(v^2 \sin^2\theta + 2\omega_0 r v \sin\theta \sin\phi + \omega_0^2 r^2)^{1/2}}\right\} \tag{12a}$$

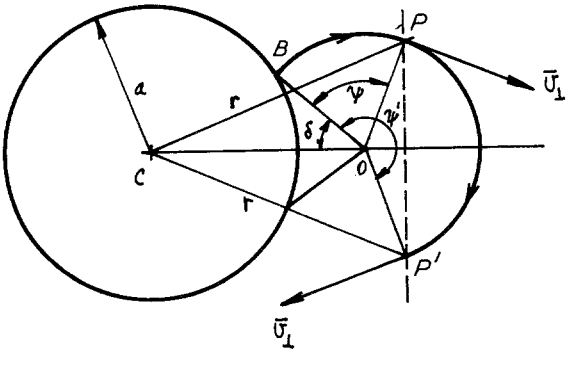

Figure 5 Symmetry conditions for scattering events that are non-tangential to the fibre surface.

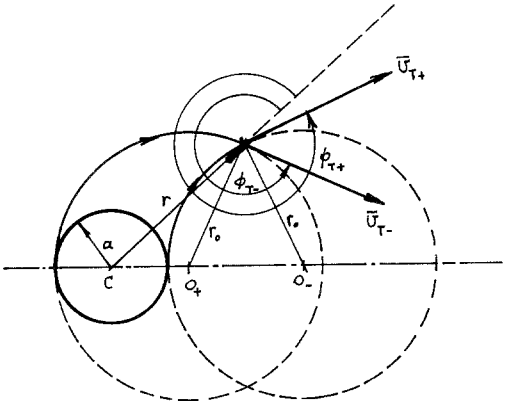

Figure 6 The tangency conditions when $a < r < 2r_0 - a$ with $r_0 > a$.

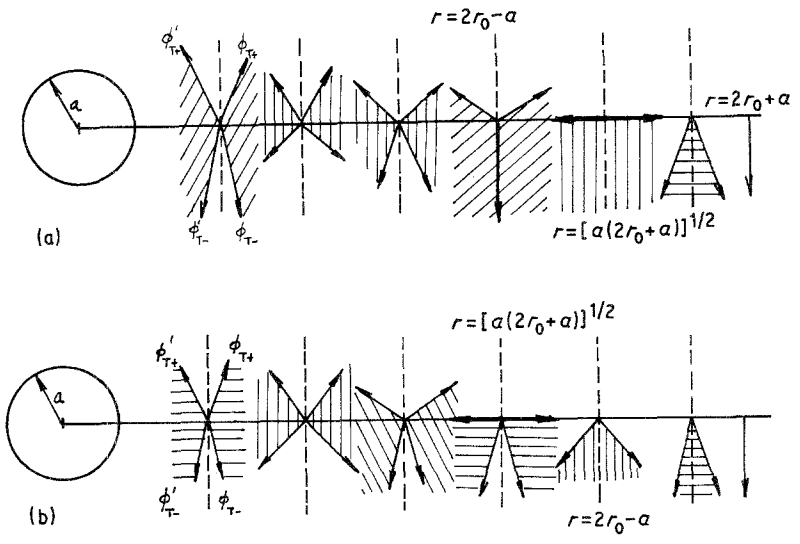

Figure 7 Regions of integration for ϕ (a) when $a < r_0 < 3a/2$ and (b) when $3a/2 < r_0$.

$$\delta = \sin^{-1}\left\{\frac{\omega_0\{a^2v^2\sin^2\theta - [rv\sin\theta\sin\phi + \frac{1}{2}\omega_0(r^2 - a^2)]^2\}^{1/2}}{v\sin\theta(v^2\sin\theta + 2\omega_0 rv\sin\theta\sin\phi + \omega_0^2 r^2)^{1/2}}\right\} \quad (12b)$$

The solution, Equation 1, to the Boltzmann equation can be written in the form

$$F^1 = \frac{eE\tau}{m^*}\frac{\partial F^0}{\partial v_z}\left\{1 - \exp\left(-\frac{R_0\psi}{\Lambda}\right)\right\} \quad (13)$$

where e is absolute value of the charge of the electron, E is the electric field, m^* is the electron effective mass, τ is the relaxation time, and F^1 is the change in the equilibrium distribution function F^0, and where $\Lambda = v\tau$ and $R_0 = v/\omega_0$. The radius of r_0 is the circular path described by the electron on the plane perpendicular to the fibre or $r_0 = R_0\sin\theta$, and $R_0\psi$ is the length of the actual helical path described by the electron.

The expression for $\Delta j(r)$ is [2]

$$\Delta j(r) = 2e\left(\frac{m^*}{h}\right)^3\int_0^\infty v^2\,dv\int\sin\theta\,d\theta\int\Delta F^1 v_z\,d\phi \quad (14)$$

where

$$\Delta F^1 = \frac{eE\tau}{m^*}\frac{\partial F^0}{\partial v_z}\exp\left(-\frac{R_0\psi}{\Lambda}\right) \quad (15)$$

and the limit of integration for θ and ϕ integrals will be determined in the next section.

The expression for j_0 is given by

$$j_0 = 2e\left(\frac{m^*}{h}\right)^3\int_0^\infty v^2\,dv\int_0^\pi\sin\theta\,d\theta\int_0^{2\pi} v_z F_b^1\,d\phi$$

where

$$F_b^1 = \frac{eE\tau}{m^*}\frac{\partial F^0}{\partial v_z}$$

is the solution to the Boltzmann equation in the region outside the scattering region. Proceeding as discussed elsewhere [2], we have

$$j_0 = 2e\left(\frac{m^*}{h}\right)^3\left(\frac{eE\tau}{m^*}\right)\frac{4}{3}\pi v_F^2 \quad (16)$$

where v_F is the Fermi velocity, and the expression for $\Delta j(r)$ is [2]

$$\Delta j(r) = 2e\left(\frac{m^*}{h}\right)^3\left(\frac{eE\tau}{m^*}\right)v_F^3\int\cos^2\theta\sin\theta\,d\theta \times\int\exp\left(-\frac{R_0\psi}{\Lambda}\right)d\phi \quad (17)$$

with $\Lambda = v_F\tau$. We can calculate the ratio $\Delta j(r)/j_0$ from Equations 16 and 17, to give

$$\frac{\Delta j(r)}{j_0} = \frac{3}{4\pi}\int\cos^2\theta\sin\theta\,d\theta\int\exp\left(-\frac{R_0\psi}{\Lambda}\right)d\phi \quad (18)$$

and substituting Equation 18 into Equation 10b, gives

$$\frac{\sigma}{\sigma_0} = (1 - V_f)\left\{1 - \frac{3}{2(1 - V_f)A_{cell}}\int_a^{r_{sc}} r\,dr \times\int\cos^2\theta\sin\theta\,d\theta\int\exp\left(-\frac{R_0\psi}{\Lambda}\right)d\phi\right. \quad (19)$$

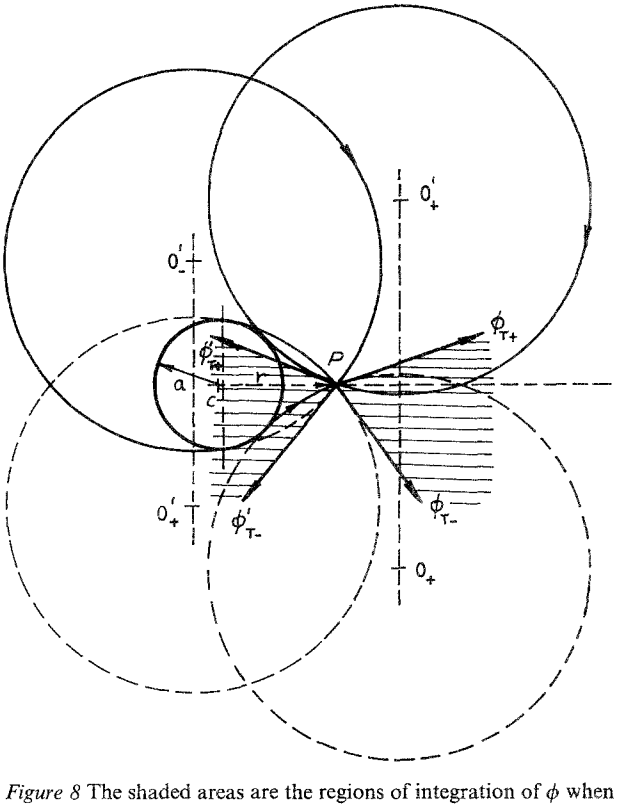

Figure 8 The shaded areas are the regions of integration of ϕ when $a < r < 2r_0 - a$.

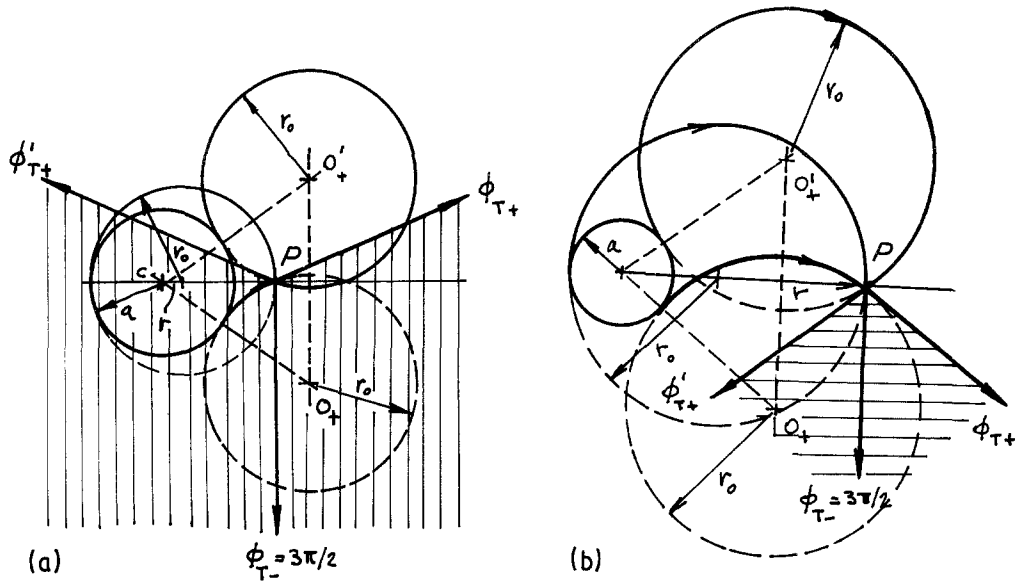

Figure 9 The shaded areas are the regions of integration of ϕ (a) when $r = 2r_0 - a$ and $a < r_0 < 3a/2$, and (b) when $r = 2r_0 - a$ and $3a/2 < r_0$.

Equation 19 gives the electrical conductivity of metal matrix composite materials in the presence of an electric and magnetic fields aligned parallel to the fibres. The next step is to compute the limits of integration of the integrals over θ and ϕ, to which we shall return shortly.

3.1. Composite conductivity without magnetic field

It was shown elsewhere [2] that in the absence of a magnetic field Equation 19 can be written in a dimensionless form using the following variables: $x = r/a$, $k = 2a/\Lambda$,

$$\frac{\sigma}{\sigma_0} = (1 - V_f)\left\{1 - (1 - p)\frac{2\pi a^2}{(1 - V_f)A_{cell}} \times \left(\frac{3}{\pi}\right)\int_1^{1+2/k} x\,dx \int_0^{\pi/2} f(\theta)\,d\theta \times \int_0^{\varphi_{max}} h(x, \theta, \varphi)\,d\varphi\right\} \quad (20)$$

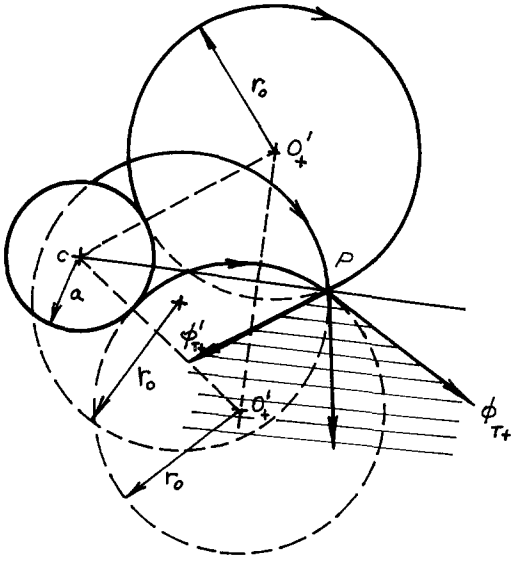

Figure 10 The shaded area in the region of integration of ϕ when $r > 2r_0 - a$.

where p is a scattering parameter to account for the effects of electrons scattering from fibre surfaces [2]. This parameter is set equal to zero because microstructural examination of the fibre surface shows that it is irregular compared to the lattice dimensions. Consequently, electrons are scattered diffusively. In Equation 20,

$$f(\theta) = \cos^2\theta \sin\theta \quad (21)$$

and

$$h(x, \theta, \varphi) = \exp\left\{-\frac{k}{2\sin\theta}[x\cos\varphi - (1 - x^2\sin^2\varphi)^{1/2}]\right\} \quad (22)$$

and $\varphi_{max} = \sin^{-1}(1/x)$. Since the volume of fibre per unit length, in the fibre direction, of cell shown in Fig. 11 is $v_f = \pi a^2$, and the total cell volume per unit length of cell is $v_t = (D + 2a)^2$, then the fibre volume fraction is $V_f = v_f/v_t = \pi a^2/(D + 2a)^2$, therefore the constant in front of the integral becomes

$$\frac{2\pi a^2}{(1 - V_f)A_{cell}} = \frac{2\pi a^2}{(1 - V_f)(D + 2a)^2} = \frac{2V_f}{1 - V_f} \quad (23)$$

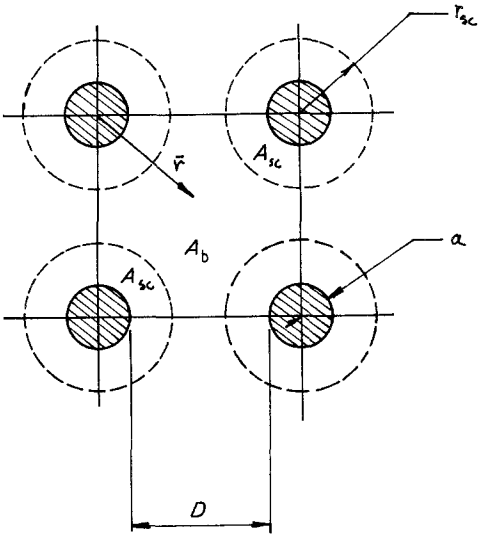

Figure 11 Model of the unit cell.

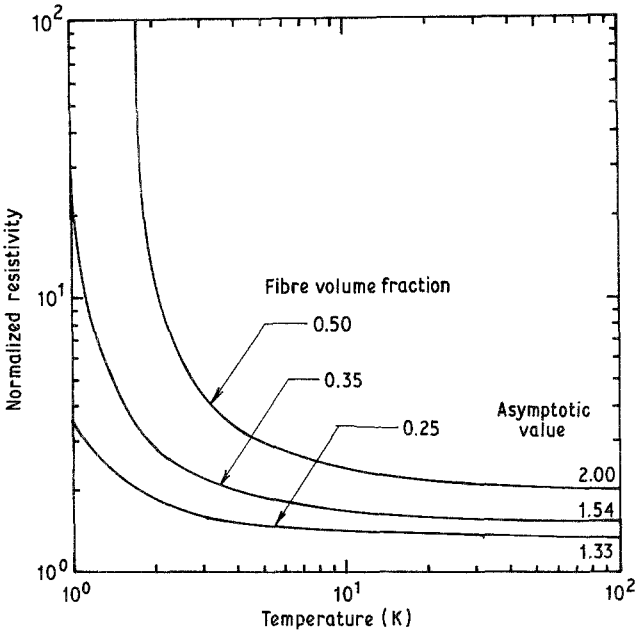

Figure 12 Normalized composite resistivity as a function of temperature at cryogenic temperatures in the absence of a magnetic field ($B = 0$).

Elsewhere [2], we discussed the numerical integration of Equation 20, which resulted in

$$I(k) = \frac{3}{\pi}\int_1^{1+2/k} x\,dx \int_0^{\pi/2} f(\theta)\,d\theta \int_0^{\varphi_{max}} h(x\theta\varphi)\,d\varphi \tag{24}$$

and it was shown that $I(k)$ is a linear function in k, so that a single repression analysis gave

$$I(k) = 0.27k^{-1.08} \tag{25}$$

To relate the conductivity to temperature, we assumed that k and T could be linearly related, and a heuristic argument showed that $T = 3k$, so that Equation 24 becomes

$$I(T) = 0.88T^{-1.08} \tag{26}$$

Combining Equations 23, 24, and 26 into Equation 20 with $p = 0$, gives

$$\frac{\sigma}{\sigma_0} = (1 - V_f)\left\{1 - 1.77\left(\frac{V_f}{1 - V_f}\right)T^{-1.08}\right\} \tag{27}$$

Elsewhere [2], Equation 27 was incorrectly derived yielding results that are too high for the composite resistivity (the resistivity $\varrho = 1/\sigma$). Fig. 12 shows the results obtained with Equation 27 for three values of the fibre volume fraction: 0.25, 0.35, and 0.50. Below about 10 K the resistivity ratio rises very sharply. As $T \to 1.697$ K for $V_f = 0.5$, $\varrho/\varrho_0 \to \infty$. In all cases, as T increases, $\sigma/\sigma_0 \to (1 - V_f)$ as it should. It can be seen that at $T \simeq 20$ K, ϱ/ϱ_0 is close to its asymptotic value of $(1 - V_f)^{-1}$.

4. Evaluation of the limits of integration

Now we proceed to discuss the evaluation of the limits of integration that have to be introduced into Equation 19 for the electrical conductivity in the presence of an electric and magnetic fields. We will distinguish two cases: $R_0 < a$ and $R_0 > a$.

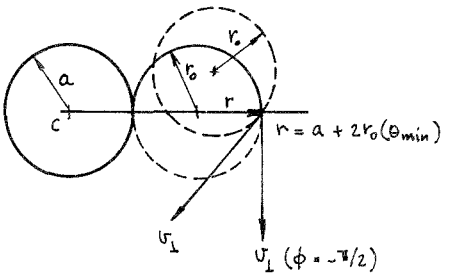

Figure 13 Conditions defining $\theta_{min}(r)$.

4.1. The case $R_0 < a$

The radius of the trajectory projected on a plane normal to the fibre is $r_0(\theta) = R_0 \sin\theta$, with $R_0 = v_F/\omega_0$, where v_F is the Fermi velocity, so that

$$R_0 = \frac{m^* v_F}{eB} \tag{28}$$

since $\omega_0 = eB/m^*$. When $R_0 < a$, we have that $r_0(\theta) < a$ for all values of θ. At $\theta = 0$, we find $v_\perp = 0$, but as θ increases, $v_\perp$ increases also, and initially the $\bar{B}$-field produces a small radius of curvature with the result that at a given position r from the centre of the fibre the trajectory does not intercept the fibre, that is, $r_0(\theta) < (r - a)/2$. When θ reaches the value $\theta_{min}(r)$ such that $r_0(\theta_{min}) = (r - a)/2$, then there is one trajectory that is tangent to the fibre and it corresponds to $\phi = -\pi/2$, shown in Fig. 13. For any other ϕ and the same $r_0(\theta_{min})$ the trajectory does not intercept the wall. Thus, we have $r_0(\theta_{min}) = R_0 \sin\theta_{min} = (r - a)/2$ from which

$$\theta_{min} = \sin^{-1}\left(\frac{r - a}{2R_0}\right) \tag{29}$$

Now, for any $\theta > \theta_{min}$ we have the shaded region shown in Fig. 14 for the integration over the variable ϕ. This region is $\phi'_{T+} \leqslant \phi \leqslant \phi_{T+}$. For θ increasing beyond θ_{min} up to a value $\theta = \pi/2$, we always obtain a valid range of integration for ϕ. When $\theta = \pi/2$, we have $v_\perp = v_F$ and there results $(r_0)_{max} = R_0$.

Now the region of integration for the radius r is from $r = a$ to $r = r_{sc}$, where $r_{sc} = a + 2R_0$ or $r_{sc} = a + D/2$. If the B-field is such that $2R_0 < D/2$, then the integration is from a to $a + 2R_0$, otherwise the integration is up to $a + D/2$. From Equation 28 if $R_0 < a$ then $B > m^* v_F/ea$ and $B_{min} = m^* v_F/ea$. For a typical B/Al metal matrix composite material, $B_{min} = 0.23T$, which is a strong field. This value assumes a fibre diameter of 0.1 mm. For any $B < B_{min}$, $R_0 > a$.

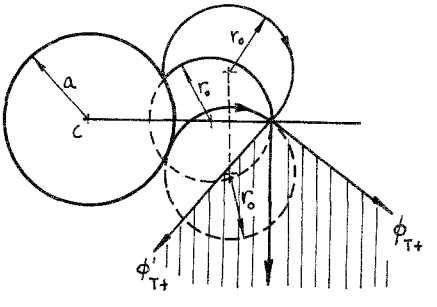

Figure 14 The shaded area in the region of integration of ϕ when $r_0 < a$.

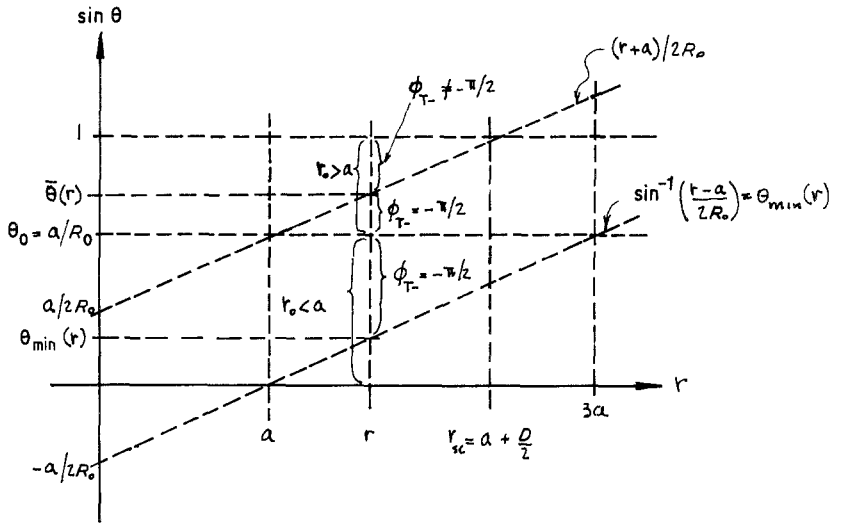

Figure 15 Definition of ϕ in the $\sin\theta$ versus r space. $a < R_0 < 2a$.

It is now necessary to make an assumption concerning the relationship between D and a. We set $D \leqslant 4a$ which corresponds to $V_f \geqslant -0.087$. ($V_f = \pi a^2/(D + 2a)^2 = \pi a^2/(4a + 2a)^2 = \pi/36 = 0.087$.) Thus a reasonable lower limit when considering that current unidirectional fibre reinforced metals have a lower value $V_f \simeq 0.20$ to 0.25. We can write $D = (4a)q$ with $q < 1$. Then, if $2R_0 \leqslant D/2$, the $\bar{B}$-field must be $B \geqslant 4m^*v_F/eD$ or $B \geqslant m^*v_f/ea(1/q) = B_{min}/qB_{min}$. Consequently, if $B \geqslant B_{min}/q$, then $r_{sc} = a + 2R_0 \leqslant a + D/2 \leqslant 3a$, and the radial integration is from $r = a$ to $r = a + 2R_0$, and if $B < B_{min}/q$ then $r_{sc} = a + D/2$.

Finally, when $R_0 < a$, the integral expression (Equation 19) for the electrical conductivity is

$$\frac{\sigma}{\sigma_0} = (1 - V_f)\left\{1 - \frac{3}{(1 - V_f)A_{cell}}\int_a^{r_{sc}} r\,dr \times \int_{\sin^{-1}[(r-a)/2R_0]}^{\pi/2} \cos^2\theta \sin\theta\,d\theta \times \int_{-\pi/2}^{\phi_{T+}(r,\theta)} (e^{-R_0\psi/\Lambda} + e^{-R_0\psi'/\Lambda})\,d\phi\right\} \quad (30)$$

where

$$\phi_{T+}(r, \theta) = -\sin^{-1}\left\{\frac{r^2 - a^2 - 2aR_0\sin\theta}{2R_0 r\sin\theta}\right\} \quad (31)$$

which follows from Equation 4 with $r_0 = R_0\sin\theta$, and ψ and ψ' are related by the symmetry of Equation 5: $\psi = \alpha - \delta$ and $\psi' = 2\pi - (\alpha - \delta)$.

If $B > B_{min}/q$, then $r_{sc} = a + 2R_0$ and we note that as $B \to \infty$, $R_0 \to 0$ so that $r_{sc} = a$, which means that $\sigma/\sigma_0 = (1 - V_f)$, which is the bulk electrical conductivity value as expected since decreasing the magnetic field causes the electron paths to have smaller and smaller radii of curvature thereby preventing collisions with fibres.

4.2. The case $R_0 > a$

There are two possibilities for $r_0(\theta)$. From $\sin\theta = r_0/R_0$ it follows that for $\theta > \sin^{-1}(a/R_0)$, $r_0(\theta) > a$; and for $\theta < \sin^{-1}(a/R_0)$, $r_0(\theta) < a$. Letting $\theta_0 = \sin^{-1}(a/R_0)$ then in the range $\theta_{min}(r) \leqslant \theta \leqslant \theta_0$, $r_0(\theta) < a$. For the $\theta_0 \leqslant \theta \leqslant \pi/2$, $r_0(\theta) > a$. We also note that with $D \leqslant 4a$ and $(r - a) \leqslant D/2$, we must have $\theta_{min} < \theta_0$. Now, r is integrated from a to $a + D/2$ since $B < B_{min}/q$.

Next, the dividing point $\bar{r}(\theta) = 2r_0(\theta) - a = 2R_0\sin\theta - a$ is considered which is shown in Fig. 7. From this figure it is readily seen that if $a < R_0 < 2a$ then for $a \leqslant \bar{r}(\theta) \leqslant a + D/2$ for $\theta_0 \leqslant \theta \leqslant \pi/2$. Therefore, according to the results summarized in Fig. 7, in the range of integration $a \leqslant r < \bar{r}(\theta)$ we use

$$\phi_{T-}(r, \theta) = -\sin^{-1}\left\{\frac{r^2 - a^2 + 2aR_0\sin\theta}{2R_0 r\sin\theta}\right\} \quad (32)$$

or what is the same $a \leqslant r \leqslant 2R_0\sin\theta - a$, meaning that $(r + a)/2R_0 < \sin\theta < 1$, and $\phi_{T-} \neq \pi/2$ can be used as given above.

If $\sin\theta < (r + a)/2R_0$, we use $\phi_{T-} = -\pi/2$, then for a given value of r between a and $a + D/2$ the range of the polar angle θ is determined and for a given r and θ the range of the azimuthal angle is also determined. This is shown in Fig. 15.

The limits for the two angular integrations are thus

$$\int_{\theta_{min}(r)}^{\theta_0} d\theta \int_{-\pi/2}^{\phi_{T+}(r,\theta)} d\phi[r_0(\theta) < a] + \int_{\theta_0}^{\bar{\theta}(r)} d\theta \int_{-\pi/2}^{\phi_{T+}(r,\theta)} d\phi[r_0(\theta) > a] + \int_{\bar{\theta}(r)}^{\pi/2} d\theta \int_{\phi_{T-}(r,\theta)}^{\phi_{T+}(r,\theta)} d\phi[r_0(\theta) > a]$$

Since the expression for $\phi_{T+}(r, \theta)$, Equation 31, for the case when $r_0(\theta) < a$ or $r_0(\theta) > a$ is the same, and the lower limit of the integration over ϕ is the same for the first two integrals, these two integrals can be lumped together so that there results

$$\int_{\theta_{min}(r)}^{\bar{\theta}(r)} d\theta \int_{-\pi/2}^{\phi_{T+}(r,\theta)} d\phi + \int_{\bar{\theta}(r)}^{\pi/2} d\theta \int_{\phi_{T-}(r,\theta)}^{\phi_{T+}(r,\theta)} d\phi \quad (33)$$

When $R_0 > 2a$, then $\bar{r}(\pi/2) = 2R_0 - a > 3a > a + D/2$ (for $D \leqslant 4a$) which is outside the region of integration for the variable r. Consequently, there is a value of θ for which $\bar{r}(\theta) = a + D/2$. This occurs when $\sin\theta = (D + 4a)/4R_0 < 1$ which is obtained from the condition that $2R_0\sin\theta - a = a + D/2$. Therefore, in the range $\theta_0 \leqslant \theta \leqslant \sin^{-1}[(D + 4a)/4R_0]$ we find that $a \leqslant \bar{r}(\theta) \leqslant a + D/2$, and in the range $\sin^{-1}[(D + 4a)/4R_0] < \theta \leqslant \pi/2$ we have $\bar{r}(\theta) \geqslant a + D/2$, which is outside the region of integration. Now recalling that whenever $r < \bar{r}(\theta)$

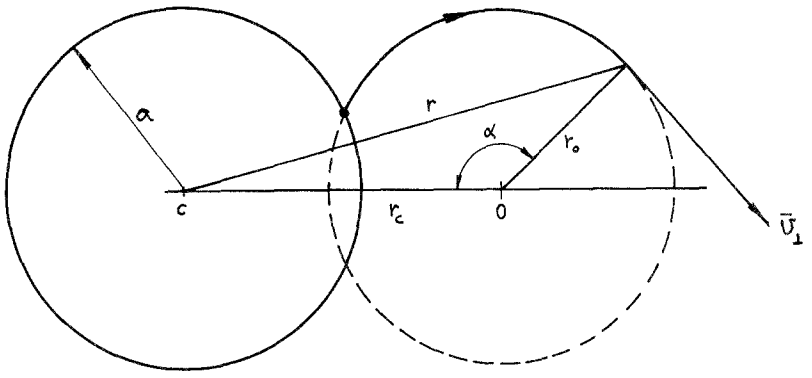

Figure 16 Definition of the angle α.

we have to use $\phi_{T-} \neq \pi/2$ for the lower limit of the integration over ϕ and $\phi_{T-} = -\pi/2$ whenever $r > \bar{r}(\theta)$, the following limits of integration obtain

$$\int_{\theta_{\min}(r)}^{\theta_0} d\theta \int_{-\pi/2}^{\phi_{T+}(r,\theta)} d\phi[r_0(\theta) < a] + \int_{\theta_0}^{\bar{\theta}(r)} d\theta \int_{-\pi/2}^{\phi_{T+}(r,\theta)} d\phi[r_0(a) > a] + \int_{\bar{\theta}(r)}^{\sin^{-1}\{D+4a/4R_0\}} d\theta \int_{\phi_{T-}(r,\theta)}^{\phi_{T+}(r,\theta)} d\phi[r_0(\theta) > a] + \int_{\sin^{-1}\{D+4a/4R_0\}}^{\pi/2} d\theta \int_{\phi_{T-}(r,\theta)}^{\phi_{T+}(r,\theta)} d\phi[r_0(\theta) > a]$$

Now, the integrals over r can be lumped together with the same limits of integration on ϕ as before and the same expression as Equation 33 is obtained.

The integral expression for the electrical conductivity, when $R_0 > a$, is

$$\frac{\sigma}{\sigma_0} = (1 - V_f)\left\{1 - \frac{3}{(1 - V_f)A_{cell}}\int_a^{a+D/2} r\,dr \times \left[\int_{\sin^{-1}\{r-a/2R_0\}}^{\sin^{-1}\{r+a/2R_0\}} \cos^2\theta \sin\theta\, d\theta \times \int_{-\pi/2}^{\phi_{T+}(r,\theta)} (e^{-R_0\psi/\Lambda} + e^{-R_0\psi'/\Lambda})\, d\phi + \int_{\sin^{-1}\{r+a/2R_0\}}^{\pi/2} \cos^2\theta \sin\theta\, d\theta \times \int_{\phi_{T-}(r,\theta)}^{\phi_{T+}(r,\theta)} (e^{-R_0\psi/\Lambda} + e^{-R_0\psi'/\Lambda})\, d\phi\right]\right\} \quad (34)$$

where $\phi_{T+}(r, \theta)$ and $\phi_{T-}(r, \theta)$ are given by Equations 31 and 32, respectively, and $\psi = \alpha - \delta$, $\psi' = 2\pi - (\alpha + \delta)$, where α and δ are given by Equation 12, respectively.

Now, when $R_0 > a$, the integrand in ϕ can be approximated as follows:

$$e^{-R_0\psi/\Lambda} + e^{-R_0\psi'/\Lambda} = e^{-R_0\psi/\Lambda}\{e^{R_0\delta/\Lambda} + e^{-2\pi R_0/\Lambda}e^{-R_0\delta/\Lambda}\}$$

with $\Lambda \leqslant D/2 \leqslant 2a$ and for $R_0 > a$ it follows that $R_0/\Lambda > 1/2$ so that $\exp(R_0\delta/\Lambda) > \exp(\delta/2)$ and $\exp[-(2\pi + \delta)R_0/\Lambda] \leqslant \exp[-(2\pi + \delta)/2] = \exp(-\pi)\exp(\delta/2) < \exp(\delta/2) < \exp(R_0\delta/\Lambda)$, and since $\exp(-\pi)\exp(\delta/2) \ll \exp(\delta/2)$ we have then $\exp[-(2\pi + a)R_0/\Lambda] \ll \exp(R_0\delta/\Lambda)$, and the term $\exp(-R_0\psi'/\Lambda)$ in front of $\exp(-R_0\delta/\Lambda)$ can be dropped. This means that the dominant term is $\exp(-R_0\psi/\Lambda)$. This is in agreement with Fig. 6 where the path length for ψ' is greater than for ψ. Therefore, we have for the electrical conductivity, when $R_0 > a$, that

$$\frac{\sigma}{\sigma_\theta} = (1 - V_f)\left\{1 - \frac{3}{(1 - V_f)A_{cell}}\int_a^{a+D/2} r dr \times \left[\int_{\theta_{\min}(r)}^{\bar{\theta}(r)} \cos^2\theta \sin\theta\, d\theta \int_{-\pi/2}^{\phi_{T+}(r,\theta)} e^{-R_0(\alpha-\delta)/\Lambda}\, d\phi + \int_{\bar{\theta}(r)}^{\pi/2} \cos^2\theta \sin\theta\, d\theta \int_{\phi_{T-}(r,\theta)}^{\phi_{T+}(r,\theta)} e^{-R_0(\alpha-\delta)/\Lambda}\, d\phi\right]\right\} \quad (35)$$

where $\theta_{\min}(r) = \sin^{-1}[(r - a)/2R_0]$ and $\bar{\theta}(r) = \sin^{-1}[(r + a)/2R_0]$ and $\phi_{T+}(r, \theta)$ and $\phi_{T-}(r, \theta)$ are given by Equations 31 and 32, respectively.

When $B \to 0$, then $R_0 \to \infty$ and $\bar{\theta}(r) \to 0$, $\theta(r) \to 0$, moreover $\lim_{R_0\to\infty} \phi_{T+} = \sin^{-1}(a/r)$ and $\lim_{R_0\to\infty} \phi_{T-} = -\sin^{-1}(a/r)$ so that

$$\lim_{R_0\to\infty} e^{-R_0\psi/\Lambda} = e^{-[r\cos\phi - (a^2 - r^2\sin^2\phi)^{1/2}]/\Lambda\sin\theta}$$

so that Equation 35 becomes

$$\frac{\sigma}{\sigma_0} = (1 - V_f)\left\{1 - \frac{6}{(1 - V_f)A_{cell}}\int_a^{a+D/2} r\,dr \times \int_0^{\pi/2} \cos^2\theta \sin\theta\, d\theta \int_0^{\sin^{-1}(a/r)} \exp\{-[r\cos\phi - (a^2 - r^2\sin^2\phi)^{1/2}]/\Lambda\sin\theta\}\, d\phi\right\} \quad (36)$$

When the following dimensionless variables are used; $x = r/a$ and $k = 2a/\Lambda$, then Equation 36 is equivalent to Equation 20, which is that derived elsewhere [2] for the case when there is no magnetic field.

Finally, one note of caution is in order: in Equation 12 for α and δ, the function $\sin^{-1}x$ is defined to be the principal branch $-\pi/2 \leqslant \sin^{-1}x \leqslant \pi/2$. In fact, α and δ can take values greater than $\pi/2$.

Consider first the case $r_0 < a$. Figure 16 shows that whenever

$$r^2 > r_c^2 + r_0^2 \quad (37)$$

then $\pi/2 < \alpha < \pi$. The expression for r_c obtained in Part I of this paper [1] is

$$r_c^2 = r^2 + r_0^2 + 2r_0 r\sin\phi \quad (38)$$

and inserting Equation 38 into Equation 37 yields

$$\sin\phi < -\frac{r_0}{r} \quad (39)$$

whenever $\pi/2 < \alpha < \pi$. In this case we have to replace α, given by Equation 12, by $\alpha \to \pi - \alpha$, and

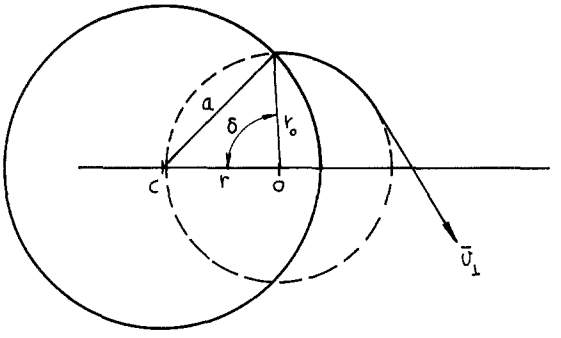

Figure 17 Definition of the angle δ.

$\alpha > \pi$ is resolved by the symmetry relation discussed above. Now, if on the other hand $\sin \phi > -r_0/r$, then $\alpha < \pi/2$.

Now, when considering δ, Figure 17 shows that $\delta > \pi/2$ whenever $a^2 > r_c^2 + r_0^2$, and inserting Equation 38, the following condition is obtained

$$\sin \phi < \frac{\alpha^2 - r^2 - 2r_0^2}{2rr_0} \tag{40}$$

If $r_0 > a$, then the same condition as shown by Equation 39 is obtained when $\alpha > \pi/2$, and now $\delta < \pi/2$ for any value of ϕ.

The condition could have been inserted into Equations 30 and 35 thereby breaking down the ϕ integrals into the appropriate ranges. Another possibility is to try and find still more symmetry in the problem and then consider only the cases $\alpha < \pi/2$ and $\delta < \pi/2$, using Equation 12 to determine the value of α and δ. The most pedestrian possibility is to insert these conditions manually into a program that calculates the integrals numerically. Equation 20 for the case when $B = 0$ was calculated numerically on a Hewlett Packard HP-41C hand held calculator [2]. However, this was not attempted for Equations 30 and 35, mainly because of the complexity of the limits of integration, and no other numerical evaluations of Equations 30 and 35 were performed.

5. Conclusion

We have derived integral expressions for the electrical conductivity of metal matrix composite materials when a magnetic field parallel to the fibres is added to a small electrical field also parallel to the fibres. The electron mean free path in the bulk metal matrix is assumed to be no greater than half the distance between fibres. Two integral expressions are obtained for the electrical conductivity. One expression applies to strong magnetic fields meaning that $R_0/a < 1$, where $R_0 = m^* v_F/eB$. When $B \to \infty$ (or equivalently $R_0 \to 0$) the integral expression reduces to the well known conductivity value $\sigma = (1 - V_f)\sigma_0$ for metal matrix composite materials with non-conducting fibres. This result is expected on physical grounds because a very strong magnetic field produces helical trajectories of very small radii, thereby decreasing the number of electrons colliding with the fibres. For weak magnetic fields, we have $R_0/a > 1$ so that the conductivity is expressed by the sum of two integrals. When $B \to 0$ (or $R_0 \to \infty$), the electrical conductivity becomes the integral expression obtained in our earlier results when there is only a longitudinal electric field [2]. In the present paper we corrected an incorrect derivation of the composite conductivity in the absence of a magnetic field published earlier [2].

References

1. F. S. ROIG and J. E. SCHOUTENS, *J. Mater. Sci.* **22** (1987) 3749–54.
2. *Idem, ibid.* **21** (1986) 2409.

Received 12 January
and accepted 1 April 1987